

InGaAs/InP hot electron transistors grown by chemical beam epitaxy

W. L. Chen, J. P. Sun, G. I. Haddad, M. E. Sherwin, G. O. Munns, J. R. East,
and R. K. Mains

Center for High Frequency Microelectronics, Department of Electrical Engineering and Computer
Science, The University of Michigan, Ann Arbor, Michigan 48109-2122

(Received 3 February 1992; accepted for publication 23 April 1992)

In this letter, we report on the dc performance of chemical beam epitaxy grown InGaAs/InP hot electron transistors (HETs). The highest observed differential β (dI_C/dI_B) is over 100. The HETs have Pd/Ge/Ti/Al shallow ohmic base contacts with diffusion lengths less than 300 Å. Furthermore, we also demonstrated ballistic transport of electrons in an InGaAs/InP HET by obtaining an energy distribution of electrons with ~ 60 meV full width at half maximum. The measured conduction band discontinuity of InGaAs/InP is 250.3 meV, which is 39.8% of the band gap difference.

Hot electron transistors (HETs) have been studied for high speed applications during the last decade, starting from GaAs/AlGaAs HETs.¹ Heiblum *et al.*² used the same material system and reported a differential α (dI_C/dI_E) = 0.9. In order to obtain an even higher α , a pseudomorphic InGaAs base device, which offered larger Γ to L valley separation, was introduced by Seo *et al.*³ They observed a differential β (dI_C/dI_B) as high as 41 at 4.2 K. Because InGaAs and InP have wider Γ to L valley separation and higher electron saturation velocity than the GaAs/AlGaAs system, the InGaAs/InP HET⁴ was predicted to have higher current gain and better switching speed.

The HET structure is difficult to fabricate because of the problems in making an ohmic contact to a narrow base region. In previous work, Cr/Au⁵ and Au/Ge/Ni⁶ systems were the most-used metals for nonalloyed base contacts. However, the base had to be heavily doped, which limited the gain of the HETs. Furthermore, the nonalloyed Cr/Au or Au/Ni/Ge contact has a high contact resistance at low temperature if the base is not heavily doped and this degrades the high frequency performance. In this study, we used a Pd/Ge/Ti/Al ohmic system to contact a thin base layer (400 Å).⁷ This ohmic system has a shallow diffusion length (< 300 Å) and shows good ohmic behavior at 80 K.

In this work, we used the InGaAs/InP material system to study the dc performance of the HETs. Moreover, an "energy spectrometer"^{1,2} technique was used to investigate the ballistic transport of electrons and measure the collector barrier height of the HETs.

The materials of this study were grown using a Varian Gen II chemical beam epitaxy (CBE) reactor. The source materials were trimethylindium, triethylgallium, 100% phosphine and 100% arsine for In_{0.53}Ga_{0.47}As and InP. All the structures were grown on (100) Fe-doped semi-insulating InP substrates at a substrate temperature of 530 °C. The typical HET structure is shown in Fig. 1.

The fabrication of the HETs was conducted by a novel self-aligned process. First, conventional photolithography was used for all of the patternings. Second, we adopted HBr/H₂O/SWBr (saturated bromine water) for nonselective mesa etching, and H₃PO₄/H₂O₂/H₂O for selective base recess. Then the Ni/Ge/Au/Ti/Au and Pd/Ge/Ti/Al system were used for the emitter (collector) and base

contacts. After the fabrication of the devices, we conducted all dc measurements of the HETs in a cryogenic cooling stage using a HP4145B system at 80 K.

When the HET is operated under forward bias mode (as shown in Fig. 2), e.g., common base configuration, small emitter current will modulate the voltage across the emitter barrier, resulting in the modulation of collector current. For the HET with a base width (W_b) = 400 Å and a base doping (N_d) = 1×10^{17} cm⁻³, the highest differential α observed was over 0.99, which corresponded to a differential β over 100. The common base I - V characteristics of this HET are shown in Fig. 3.

We studied the dc performances of the HETs by changing the base width (W_b) and base doping (N_d). We found that as W_b and N_d were decreased, the probability of scattering was decreased, thus the differential α was increased. However, when N_d is increased, the output conductance of the HET is decreased, and the surface depletion depth is also decreased at the extrinsic base region, although the differential β is decreased. Thus, we could obtain better I - V characteristics from the HET. For $N_d = 2 \times 10^{17}$ cm⁻³, $W_b = 400$ Å (UMA-580), the common emitter I - V characteristics are shown in Fig. 4.

As shown in Fig. 4, for every I_B step, I_C dramatically increases roughly at $V_{CE} = 1.0$ V. This could be the combined effects of (1) tunneling of base electrons through the

layer	doping (cm ⁻³)	width (nm)	
InGaAs	1.0×10^{18}	300	Emitter
InGaAs	undoped	5	Spacer
InP	undoped	17.5	Emitter barrier
InGaAs	undoped	5	Spacer
InGaAs	Nd	$W_b - 10$	Base
InGaAs	undoped	5	Spacer
InP	undoped	200	Collector barrier
InGaAs	undoped	5	Spacer
InGaAs	1.0×10^{18}	400	Collector
InP buffer layer			
Fe - doped Semi - insulating InP substrate			

FIG. 1. The HET structure with base width W_b and base doping N_d .

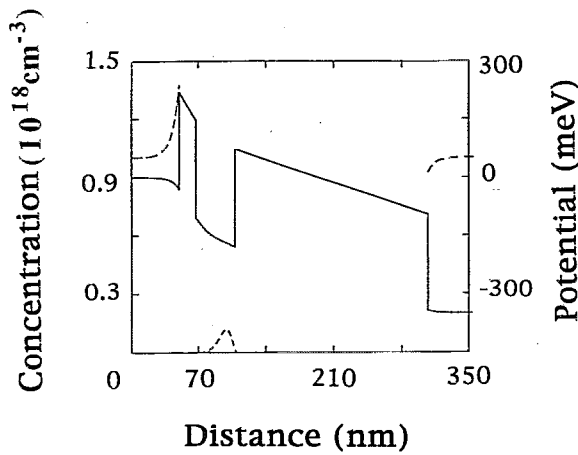


FIG. 2. The band diagram of the HET under forward bias mode, which is generated by a self-consistent simulation, solid line=conduction band, dashed line=electron concentration.

collector barrier and (2) depletion of base charge (punch through). Moreover, the HET has an I_C turn-on voltage $V_{CE} \sim 0.2$ V. Below this voltage, the emitter and collector barriers block low energy electrons efficiently, resulting in very small I_C output current. The differential β is from 32 to 45 for most of the bias range, and the highest differential β is 66. Moreover, we found that further increasing of N_d ($> 3 \times 10^{17} \text{ cm}^{-3}$) and W_b resulted in a decrease of differential β and α .

One of the advantages of studying HETs is to provide information about ballistic transport of electrons in semiconductors. Previous researchers have demonstrated this phenomenon in GaAs/AlGaAs,¹ InGaAs/AlGaAs,² and InAlAs/InGaAs⁸ HETs. In this study, we demonstrated this phenomenon in an InGaAs/InP HET for the first time with the UMA-555 HET, using an energy spectrometer technique.

For the HET operating in the energy spectrometer mode, which implies that both V_{EB} and V_{CB} are negative, the energy band diagram is shown in Fig. 5. The derivative of I_C with respect to V_{CB} , i.e., dI_C/dV_{CB} is proportional to

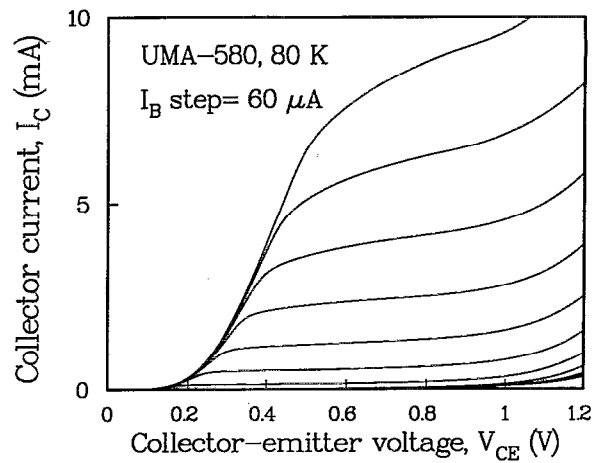


FIG. 4. Common emitter I - V characteristics of the UMA-580 HET.

the number of collected electrons as a function of energy. By varying V_{CB} , we will get a distribution of the collected electrons, as shown in Fig. 5. The main peak of this distribution is the ballistic peak² and the peak value is at $V_{CB} = V_p$. The full width at half-maximum (FWHM) of the distribution remains around 60 meV for different V_{EB} .

As discussed in Refs. 2 and 8, we can estimate the collector barrier height Φ_C from the ballistic condition, as

$$qV_{EB} - \Delta = \Phi_C + qV_{CB}(\text{at peaks}) - \delta_c - \xi. \quad (1)$$

Basically, this condition implies the energy conservation of ballistic electrons for the entire transport. Where V_{EB} is the injection voltage; Δ is the small displacement of the normal distribution peak injected into the base down from the Fermi level in the emitter; Φ_C is the collector barrier height; V_{CB} (at peak) is equal to V_p ; δ_c is the band bending at the collector side of the spectrometer barrier at $V_{CB} = V_p$; and $\xi = E_F - E_C$ is assumed to be 82.5 meV for $n_c = 1 \times 10^{18} \text{ cm}^{-3}$ at 80 K.

In Eq. (1), the V_{EB} and V_{CB} are measured values, and the Δ and δ_c are calculated by a HET simulation with an

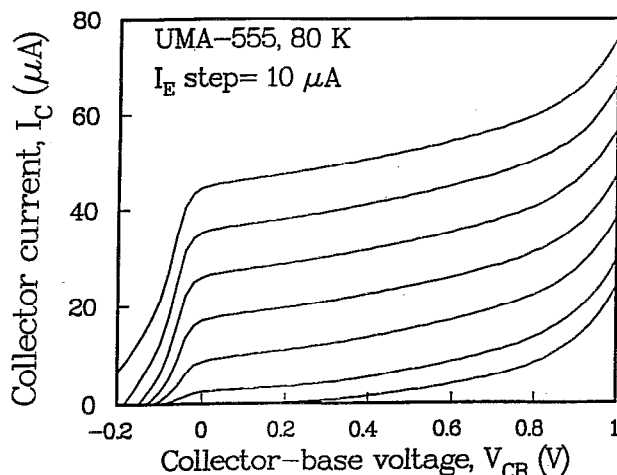


FIG. 3. Common base I - V characteristics of the UMA-555 HET.

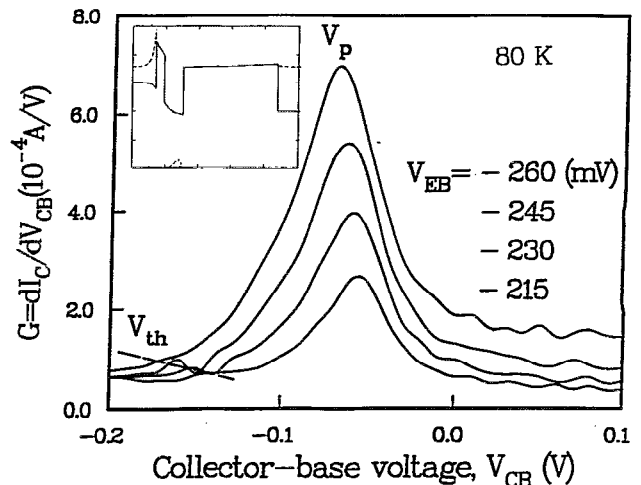


FIG. 5. G vs V_{CB} curve; and the band diagram under the energy spectrometer mode, solid line=conduction band, dashed line=electron concentration.

TABLE I. Summary of energy distribution results.

$-V_{EB}$ (mV)	Δ (meV)	δ_C (meV)	$-V_p$ (mV)	Φ_C (meV)	$-V_{th}$ (mV)
215	11.0	0.5	50	237	142.5
230	10.0	0.8	57.5	245.8	150
245	8.9	1.0	65	254.6	160
260	7.5	1.5	72.5	264	172.5

assumed barrier height of 250 meV. These values are listed in Table I for various bias conditions. The Δ becomes smaller as V_{EB} increases to more negative values, since emitter electrons see a thinner triangular emitter barrier, resulting in less reflection of electrons and a smaller Δ . From Eq. (1), the calculated collector barrier height ranges from 237 to 264 meV with an average of 250.3 meV. It agrees well with the number assumed in the HET simulation (250 meV). Moreover, the Fermi level is assumed almost at the conduction band edge in the base region. Therefore, the above result suggests that the conduction band discontinuity is 39.8% of the band gap difference for the InP/InGaAs heterojunction, and it is consistent with previous reports^{9,10} which obtained the data from admittance spectroscopy or C - V measurements.

The FWHM of the distribution is not broadened for different V_{EB} and the peak value satisfies the ballistic condition [Eq. (1)] within the energy associated with an optical phonon scattering (34.5 meV for InGaAs). Moreover, for the V_{EB} 's shown in Fig. 5, we measured the base transport ratio α (I_C/I_E) at $V_{CB}=V_p$ to determine the fraction of ballistic electrons. From the two conditions and measured α 's, we found that up to 50% of emitter electrons could travel through the base region ballistically.

Furthermore, it is shown in Fig. 5 that the G (dI_C/dV_{CB}) value does not drop to zero within the voltage range shown in Fig. 5; e.g., we find I_C drops below zero at a

threshold voltage V_{th} . This is because, when $V_{CB} < V_{th}$, electrons start to tunnel through the collector barrier from the collector to the base, resulting in negative I_C . If I_C remains unchanged for a range of voltage, dI_C/dV_{CB} will drop to zero. However, we did not observe such a range of voltage in our HET structure.

In conclusion, we have fabricated CBE grown InGaAs/InP HETs with high current gains and shallow ohmic base contacts. The processing technique developed in this study can be used to fabricate other types of resonant tunneling transistors with direct contact to the base. The InP/InGaAs material system is promising for high speed device applications. Moreover, the HET is a good tool to investigate carrier transport in semiconductors and physical properties of semiconductors.

This work was supported by the Army Research Office under the URI program Contract No. DAAL03-87-K-0007.

- ¹N. Yokoyama, K. Imamura, T. Ohshima, N. Nishi, S. Muto, K. Kondo, and S. Hiyamizu, IEEE Digest IEDM 532 (1984).
- ²M. Heiblum and M. V. Fischetti, in *Physics of Quantum Electron Devices*, edited by F. Capasso (Springer, Berlin, 1990), Chap. 9.
- ³K. Seo, M. Heiblum, C. M. Knoedler, J. E. Oh, J. Pamulapati, and P. Bhattacharya, IEEE Electron Device Lett. EDL-10, 73 (1989).
- ⁴S. Yamaura, Y. Miyamoto, and K. Furuya, Electron. Lett. 26, 1055 (1990).
- ⁵K. Uesaka, S. Yamaura, Y. Miyamoto, and K. Furuya, Electron. Lett. 25, 705 (1989).
- ⁶I. Hase, K. Taira, H. Kawai, T. Watanabe, K. Kaneko, and N. Watanabe, Electron. Lett. 24, 279 (1988).
- ⁷W. L. Chen, J. P. Sun, G. I. Haddad, M. E. Sherwin, G. O. Munns, J. R. East, and R. K. Mains, Proceedings of the 1991 International Semiconductor Devices Research Symposium, Charlottesville, VA, p. 297.
- ⁸U. K. Reddy, J. Chen, C. K. Peng, and H. Morkoc, Appl. Phys. Lett. 48, 1799 (1986).
- ⁹D. V. Lang, M. B. Panish, F. Capasso, J. Allam, R. A. Hamm, and A. M. Sergeant, J. Vac. Sci. Technol. B 5, 1215 (1987).
- ¹⁰M. T. Furtado, M. S. S. Loral, A. C. Sachs, and P. J. Shieh, Superlatt. Microstruct. 5, 507 (1989).